ELECTRONIC SUPPLEMENTARY INFORMATION

Delocalized Hole Transport Coupled to Sub-ns Tryptophanyl Deprotonation Promotes Photoreduction of Class II Photolyases

Fabien Lacombat,[a] Agathe Espagne,[a] Nadia Dozova,[a] Pascal Plaza,*[,a] Elisabeth Ignatz,[b] Stephan Kiontke,[b] Lars-Oliver Essen*[,b]

[a] *PASTEUR, Département de chimie, École normale supérieure, PSL University, Sorbonne Université, CNRS, 75005 Paris, France. E-mail: pascal.plaza@ens.fr*
[b] *Department of Chemistry, LOEWE Center for Synthetic Microbiology, Philipps University, 35032 Marburg, Germany. E-mail: essen@chemie.uni-marburg.de*

Contents

S1. Steady-state absorption spectra

The steady-state absorption spectra of the *Mm*CPDII samples used for the transient absorption experiments are reproduced in Figure S1A (normalized views are shown in Figure S1B). They essentially exhibit the characteristic bands of FAD_{ox},[1-3] peaking here at 377 ($S_0 \rightarrow S_2$ transition) and 444 nm ($S_0 \rightarrow S_1$ transition). These bands show further vibrational structures, due to the rigid environment of the molecule within the protein, in contrast with the much smoother shape of the same bands in solution.[4] No substantial presence of $FADH^{\bullet}$, characterized by distinctive peaks around 590 and 635 nm,[1-3] can be appreciated in the red part of the spectrum. Given that the S_0S_1 band is slightly more intense than the S_0S_2 band as in pure FAD_{ox} samples, it may be inferred that the amount of $FADH^{-}$, characterized by an absorption band growing below 450 nm,[4,5] is rather low.

Using a commonly admitted value of absorption coefficient of FAD_{ox} at the maximum of its $S_0 \rightarrow S_1$ transition (11300 $M^{-1}cm^{-1}$),[6] the concentration of FAD_{ox} is estimated to *ca.* 145 µM in the case of the WT sample in H_2O buffer, 109 µM for WT in D_2O and 278 µM for Y345F in H_2O.

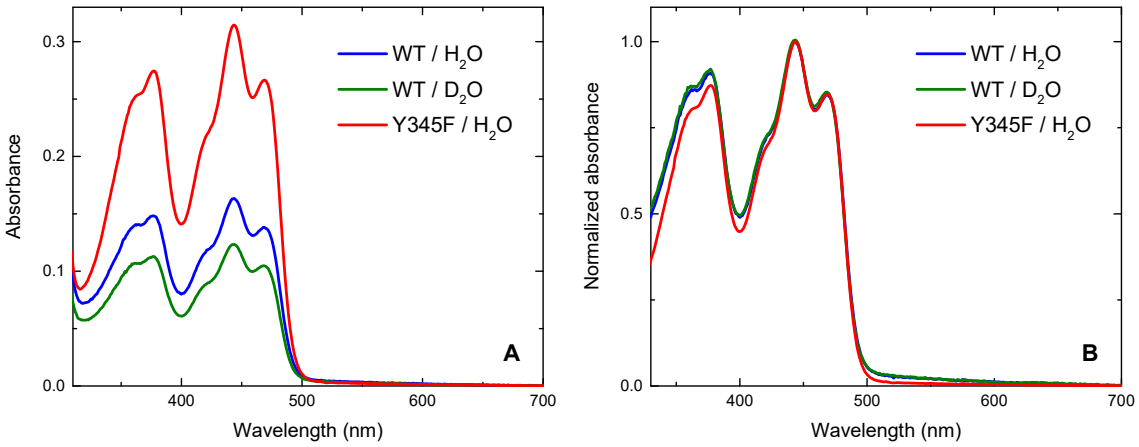

Figure S1. (A) Steady-state absorption spectrum (optical path = 1 mm) of the *Mm*CPDII samples used for the transient absorption experiments: WT in H_2O buffer in blue, WT in D_2O in green and Y345F in H_2O in red line. (B) Same spectra arbitrarily normalized at 444 nm.

S2. Transient absorption and anisotropy spectra

S2.1. WT and Y345F in H_2O buffer

The isotropic transient absorption spectra of *Mm*CPDII in H_2O buffer were given in the main text for both WT and Y345F (Figure 2). The corresponding transient anisotropy spectra, calculated from the same parallel and perpendicular transient absorption spectra, are here shown in Figure S2.

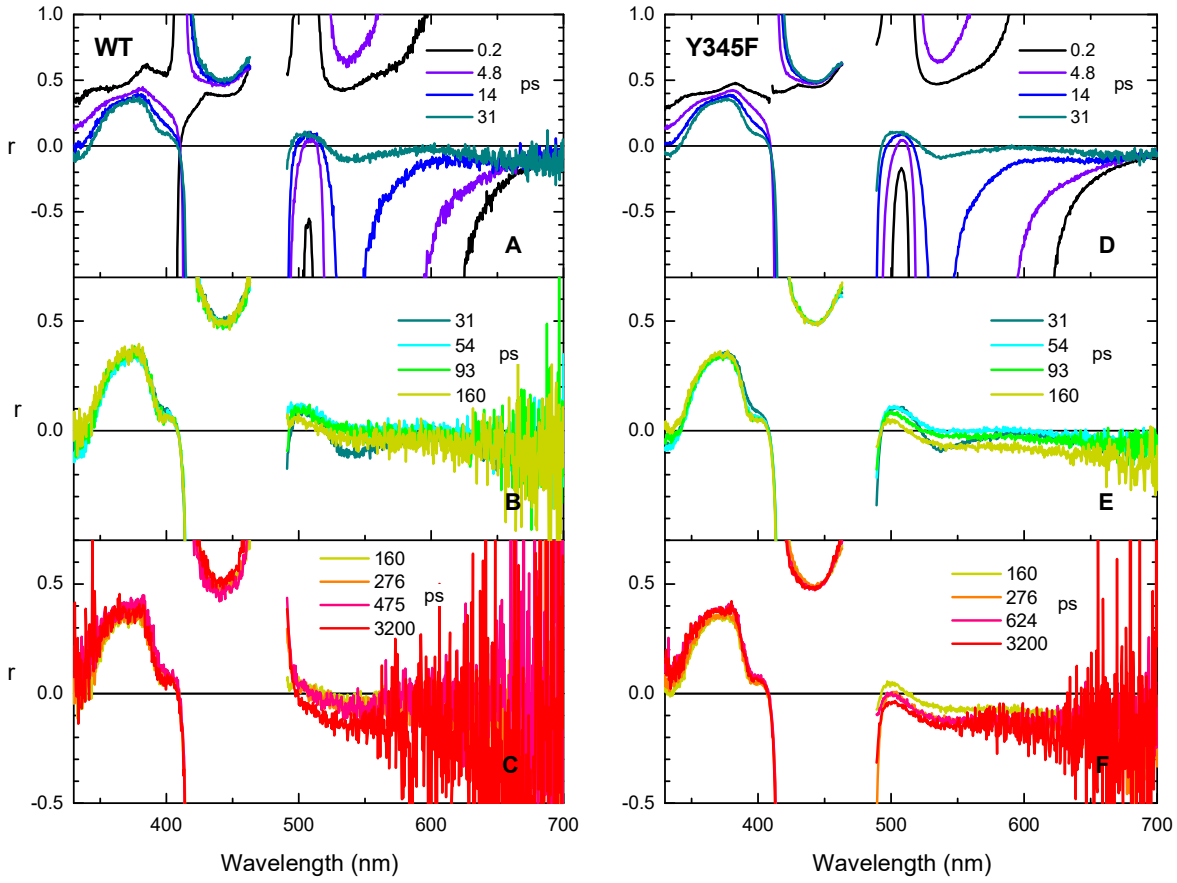

Figure S2. Transient anisotropy (r) of *Mm*CPDII in H_2O buffer, at selected pump-probe delays. WT is shown in panels A-C and Y345F in panels D-F.

S2.2. WT in D_2O buffer

The isotropic transient absorption spectra and transient anisotropy spectra of WT-*Mm*CPDII in D_2O buffer are shown in Figure S3.

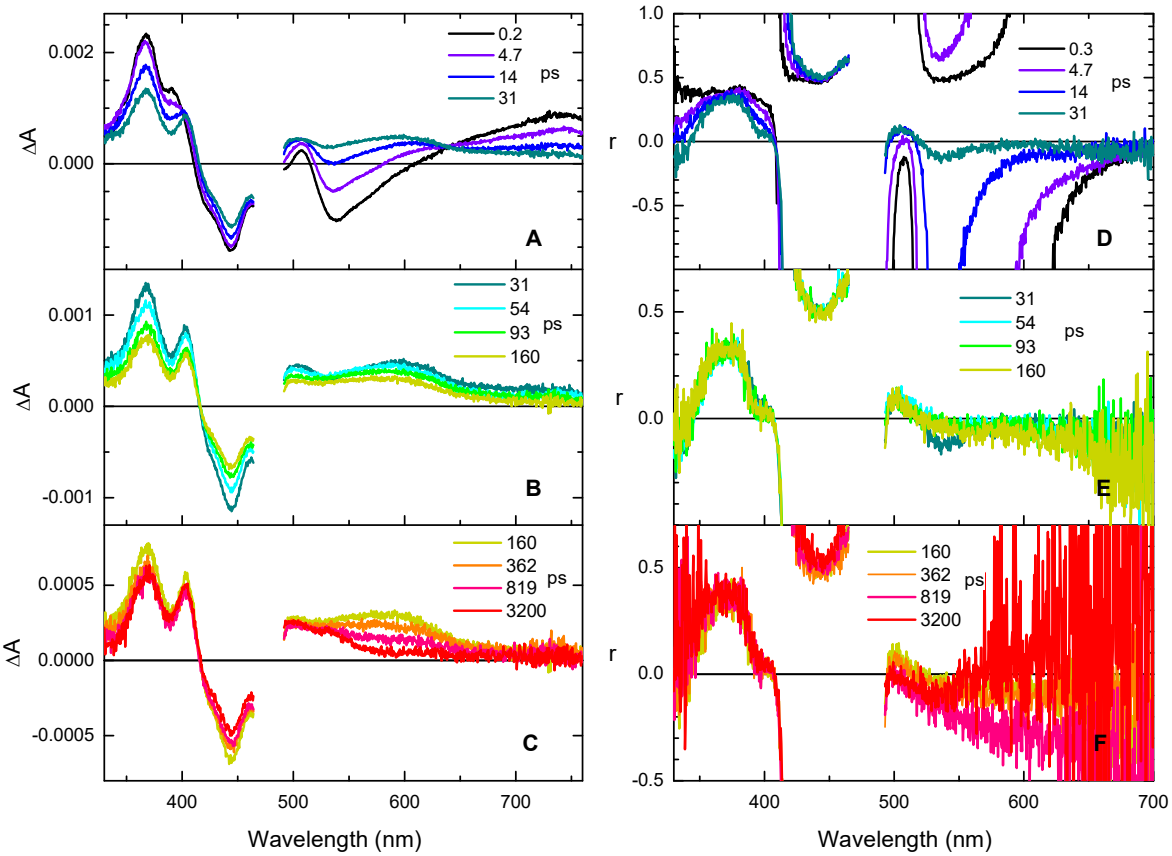

Figure S3. (A-C) Isotropic transient absorption spectra of *Mm*CPDII in D_2O buffer, at selected pump-probe delays, after fs excitation at 475 nm. (D-F) Corresponding transient anisotropy spectra.

S3. Global kinetic analysis

S3.1. Example fits

Figure S4 demonstrates the quality of the global multiexponential fits performed on the polarized transient absorption data. The kinetic traces of both isotropic transient absorption and transient anisotropy of WT-*Mm*CPDII in H_2O buffer are here shown at selected wavelengths, together with their corresponding fits. Similar qualities were obtained for the other two studied systems (WT in D_2O buffer and Y345F in H_2O buffer; not shown).

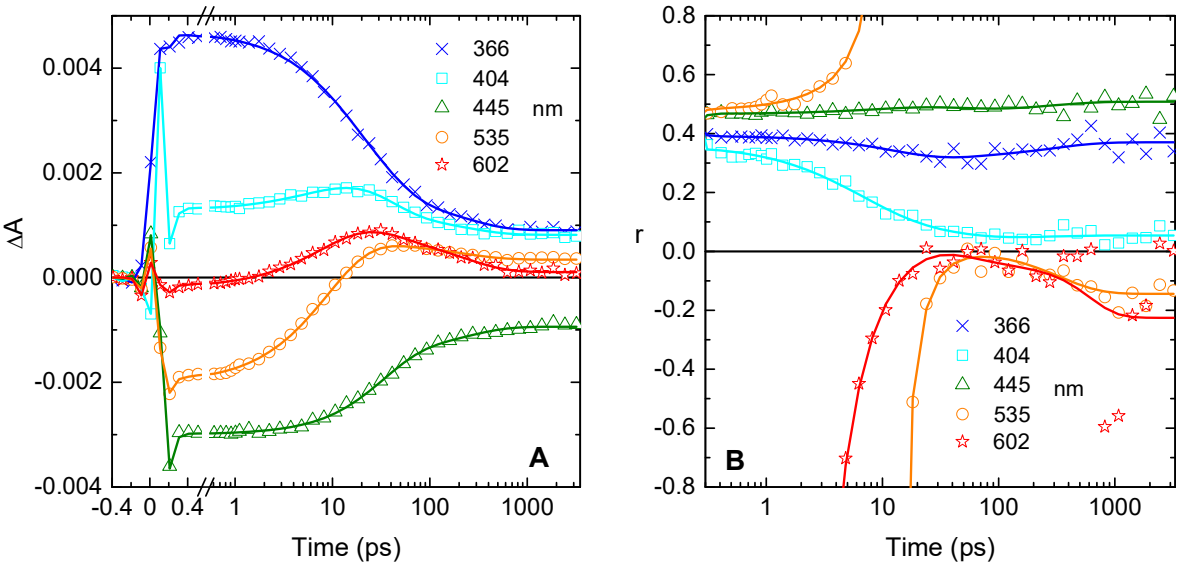

Figure S4. Kinetic traces of isotropic transient absorption (A) and transient anisotropy (B) of WT-*Mm*CPDII, at selected wavelengths. The continuous lines are effective fits deduced from the root fit of the polarized transient absorption data.

Figure S5 compares the normalized transient absorption kinetic traces of WT-MmCPDII at 602 nm, in H_2O and D_2O, to illustrates the clear kinetic isotope effect on the slow decay.

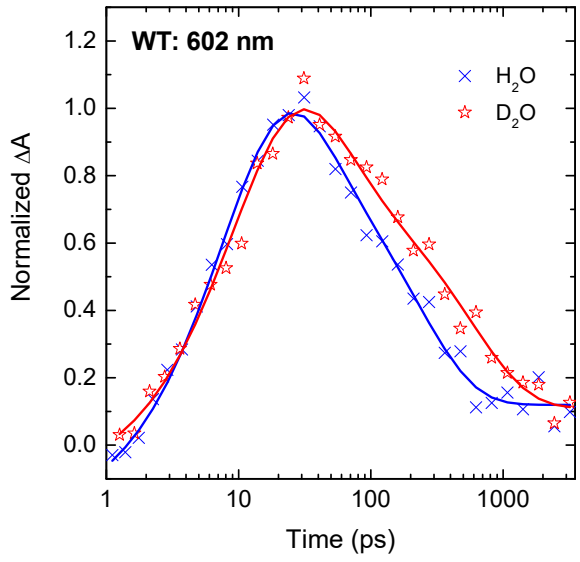

Figure S5. Comparison of the normalized transient absorption kinetic traces of WT-*Mm*CPDII at 602 nm, in H_2O (blue crosses) and D_2O (red stars). The continuous lines are effective fits deduced from the root fit of the polarized transient absorption data.

S3.2. WT in D_2O buffer

Figure S6A shows the isotropic EADS relative to the global analysis of the transient absorption spectra of WT-*Mm*CPDII in D_2O buffer. The corresponding EAAS are shown in Figure S6B.

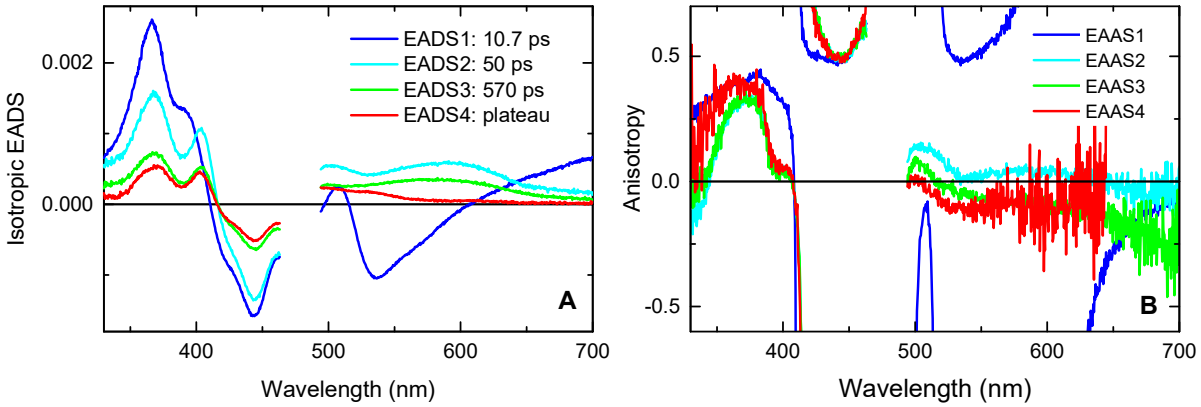

Figure S6. (A) Isotropic EADS deduced from the global analysis of the transient absorption spectra of WT-*Mm*CPDII in D_2O buffer. (B) Corresponding EAAS. Exceedingly noisy parts of EAAS4 above 645 nm have been masked.

S4. Spectral fitting

S4.1. Reference absorption spectra

In order to identify the photoproducts obtained after decay of the excited state and analyze the isotropic EADS resulting from the global analysis of the data, we used a number of reference absorption spectra taken from the literature and gathered in Figure S7. The spectrum of $FAD^{\bullet-}$ is taken from the work of Berndt et *al.* on *Drosophila* cryptochrome;[7] the spectra of $WH^{\bullet+}$, $W^{\bullet}$ come from Solar *et al.*;[8] the $YO^{\bullet}$ spectrum is taken from Aubert *et al.*[9] The FAD_{ox} spectrum represented in Figure S7 is simply that of WT-*Mm*CPDII, scaled to $\varepsilon = 11300\ M^{-1}\ cm^{-1}$ at 444 nm,[6] assuming FAD_{ox} is the dominant FAD species in presence.

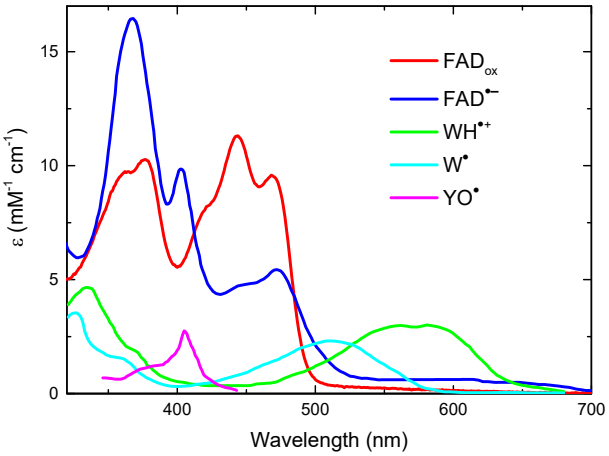

Figure S7. Reference spectra used to analyze the photoproduct spectra (see text above).

S4.2. EADS3 (WT)

The isotropic EADS3 of WT in H_2O buffer was fitted with a weighted sum of reference spectra (see SI-4.1), modified with two adjustable parameters (s, k) as shown in Equation S1 (see details in the main text, §2.5). A shift of the FAD_{ox} bleaching contribution (s_3) was introduced to take into account differences between the calibration of the steady-state and transient-absorption spectrometers. The fit is shown in the main text (Figure 4A), the optimized parameters in Table S1 and the modified reference spectra in Figure S8A. The coefficient of determination (R^2) was 0.992905.

$$\mathrm{EADS3}(\lambda) = a_1\,\varepsilon_{FAD^{\bullet-}}\big(k_1(\lambda - s_1)\big) + a_2\,\varepsilon_{WH^{\bullet+}}\big(k_2(\lambda - s_2)\big) - a_3\,\varepsilon_{FAD_{ox}}(\lambda - s_3) \qquad \text{(S1)}$$

The amplitudes (a_1, a_2, a_3) should basically represent concentrations of the involved species (multiplied by the optical path, namely 0.1 cm) but may in fact contain an implicit coefficient globally modifying the intensity of each reference spectra. Conservation relations between them should therefore not be sought.

Table S1. Optimized parameters of the fit of EADS3 (WT/H_2O) according to Equation S1.

Species	Parameter	Estimate	Standard error
$FAD^{\bullet-}$	$a_1 \times 10^4$	2.22	0.02
	s_1 (nm)	-6.35	0.93
	k_1	0.976	0.003
$WH^{\bullet+}$	$a_2 \times 10^4$	2.17	0.02
	s_2 (nm)	-86.3	3.4
	k_2	0.853	0.005
FAD_{ox}	$a_3 \times 10^4$	2.15	0.02
	s_3 (nm)	2.0	0.2

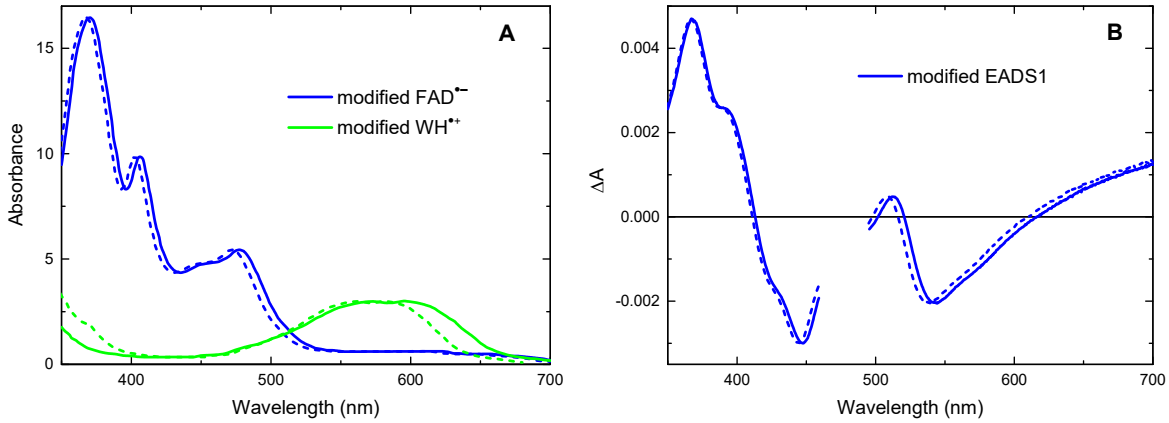

Figure S8. Modified spectra used to fit EADS3 (WT/H_2O) according to Equation S1 (A) and Equation S2 (B). The original spectra are recalled in dotted lines.

It may be noted from Figure S8 that $FAD^{\bullet-}$ has a small contribution at 600 nm, where the anisotropy measurements were taken to access the orientations of the $WH^{\bullet+}$ radicals. The relative contribution of $WH^{\bullet+}$ to the total absorbance of a $FAD^{\bullet-}/WH^{\bullet+}$ pair would accordingly amount to only 0.83 at 600 nm.

S4.3. Difference between EADS2 and EADS3 (WT)

EADS3 was here fitted with a weighted sum of EADS2 and EADS1, according to Equation S2. A shift (s_2) and scaling (k_2) of EADS1 was allowed to take into account a possible difference of excited FAD_{ox} spectrum in EADS1 and EADS2 (the fit remains however quite acceptable without any modification of EADS1). The fit is shown in the main text (Figure 4B), the optimized parameters in Table S2 and the modified EADS1 spectrum in Figure S8B. The coefficient of determination (R^2) was 0.998236.

$$\mathrm{EADS3}(\lambda) = \phi\ \mathrm{EADS2}(\lambda) - a_1\ \mathrm{EADS1}\big(k_1(\lambda - s_1)\big) \qquad \text{(S2)}$$

The modified EADS1 exhibits a slight red shift of the SE band, which might be interpreted as arising from a dielectric relaxation occurring during the 9.2-ps phase in the sub-pool of slowly reacting excited flavins. The apparent shift of the GSB band is probably meaningless and due to the limited capabilities of the spectral modification implemented in Equation S2. Parameter a_1 is interpreted as the fraction of the initial excited FAD_{ox} population still present in EADS2 but absent in EADS3. Parameter ϕ (61%) represents the fraction of transient population in EADS2

still present in EADS3, that is, the yield of the forward process. Correlatively 1- ϕ (39%) is the yield of the backward reaction, restoring the initial configuration by charge recombination of the $FAD^{\bullet-}/WH^{\bullet+}$ pair.

Table S2. Optimized parameters of the fit of EADS3 (WT/H_2O) according to Equation S2.

Spectrum	Parameter	Estimate	Standard error
EADS2	ϕ	0.612	0.002
	a_1	0.080	0.001
EADS1	s_1 (nm)	-7.3	0.9
	k_1	0.978	0.002

S4.4. Difference between EADS3 and EADS4 (WT)

EADS4 was first fitted with a weighted sum of EADS3 and a difference of $W^{\bullet}$ and $WH^{\bullet+}$ spectra, according to Equation S3. The fit is shown in the main text (Figure 4C), the optimized parameters in Table S3 and the modified reference spectra in Figure S9A. The coefficient of determination (R^2) was 0.993915.

$$\mathrm{EADS4}(\lambda) = \phi\,\mathrm{EADS3}(\lambda) - a_1\,\varepsilon_{WH^{\bullet+}}\left(k_1(\lambda - s_1)\right) + a_2\,\varepsilon_{W^{\bullet}}\left(k_2(\lambda - s_2)\right) \qquad \text{(S3)}$$

Parameter ϕ is interpreted as the fraction of the transient population present in EADS3 that undergoes further reaction, namely deprotonation of $WH^{\bullet+}$, represented by the last two terms of Equation S3; (1- ϕ) is thus the yield of charge recombination occurring in competition during the EADS3→EADS4 step.

Table S3. Optimized parameters of the fit of EADS4 (WT/H_2O) according to Equation S3.

Spectrum	Parameter	Estimate	Standard error
EADS3	ϕ	0.695	0.003
	$a_1 \times 10^4$	1.42	0.02
$WH^{\bullet+}$	s_1 (nm)	-42	2
	k_1	0.903	0.003
	$a_2 \times 10^4$	0.93	0.02
$W^{\bullet}$	s_2 (nm)	45	4
	k_2	1.09	0.01

A better fit (R^2=0.995845) could be obtained with an additional $YO^{\bullet}$ component (Equation S4). The fit is shown in the main text (Figure 4D), the optimized parameters in Table S4 and the modified reference spectra in Figure S9B.

$$\mathrm{EADS4}(\lambda) = \phi\ \mathrm{EADS3}(\lambda) - a_1\,\varepsilon_{WH^{\bullet+}}\left(k_1(\lambda - s_1)\right) + a_2\,\varepsilon_{W^{\bullet}}\left(k_2(\lambda - s_2)\right) + a_3\,\varepsilon_{YO^{\bullet}}\left(k_3(\lambda - s_3)\right) \quad \text{(S4)}$$

Table S4. Optimized parameters of the fit of EADS4 (WT/H_2O) according to Equation S4.

Spectrum	Parameter	Estimate	Standard error
EADS3	ϕ	0.678	0.003
$WH^{\bullet+}$	$a_1 \times 10^4$	1.37	0.02
	s_1 (nm)	-37	2
	k_1	0.909	0.003
$W^{\bullet}$	$a_2 \times 10^4$	0.89	0.02
	s_2 (nm)	44	4
	k_2	1.09	0.01
$YO^{\bullet}$	$a_3 \times 10^4$	0.52	0.04
	s_3 (nm)	214	17
	k_3	2.2	0.2

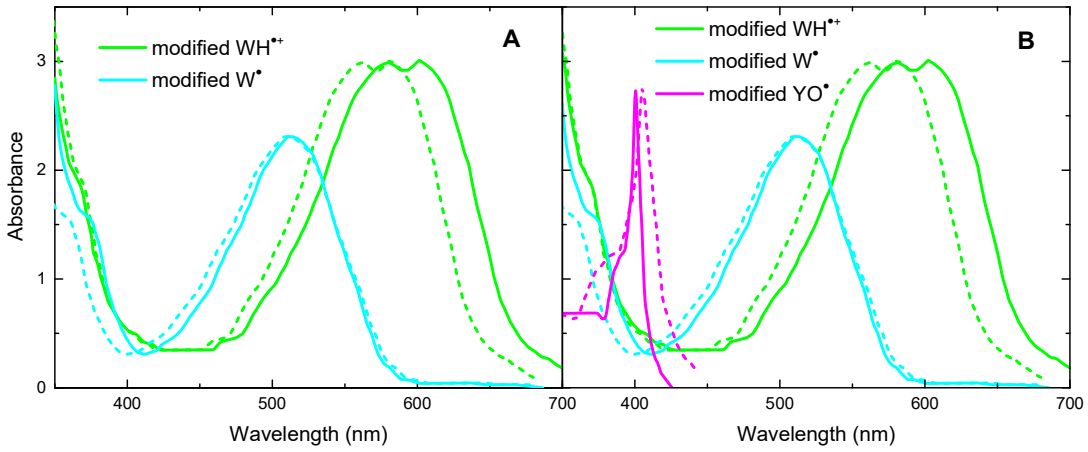

Figure S9. Modified reference spectra used to fit EADS4 (WT/H_2O) according to Equation S3 (A) and Equation S4 (B). The original spectra are recalled in dotted lines.

According to this last fit, the quantum yield of forward reaction during the EADS3→EADS4 step is 68% (ϕ). Neglecting the implicit modifications of absorption coefficients of the reference spectra, one may use the parameters of Table S4 to crudely estimate the quantum yields of tryptophanyl deprotonation (ϕ_{td}) and tyrosine oxidation (ϕ_{to}). One tentatively gets $\phi_{td} \approx \phi\ a_2/(a_2 + a_3) = 43\%$ and $\phi_{to} \approx \phi\ a_3/(a_2 + a_3) = 25\%$ (the fact that a_2+a_3 is very close to a_1 supports this approximate calculation). Accordingly, the rate of tryptophanyl deprotonation may be estimated to $k_{td} = \phi_{td}/\tau_3 = 1.9\ ns^{-1}$ and that of tyrosine oxidation to $k_{to} = \phi_{to}/\tau_3 = 1.1\ ns^{-1}$. These numbers should of course be taken with care, as mere indicators of orders of magnitude.

Finally, it may be observed that the spectral fit of EADS3 (§S4.2) did not yield identical parameters for $WH^{\bullet+}$ as that of EADS4, although the same trends (red shift and broadening of the original spectrum) are conserved. It should however be noted that the first one is not a differential fit. It involves FAD_{ox} and $FAD^{\bullet-}$ and its purpose was to demonstrate that EADS3 results from the electron transfer from a tryptophan residue to FAD, as explained in §4.2.1 of the main text. The second one focuses on the difference between EADS3 and EADS4, charge recombination being excluded. This is the only approach that can uncover the minor production of $YO^{\bullet}$. The full fit of EADS4 is indeed not reliable as it involves an exceedingly long list of contributors, some of them having ambiguously overlapping spectra ($FAD^{\bullet-}$ and $YO^{\bullet}$). The difference of approach may justify the differences obtained for the modified $WH^{\bullet+}$ spectrum.

S4.5. Difference between EADS3 and EADS4 (Y345F)

The spectral fit of EADS4 according to Equation S3 was repeated for Y345F. The fit and the modified reference spectra are shown in Figure S10. The optimized parameters are listed in Table S5. The coefficient of determination (R^2) was 0.996754. No better fit was obtained by adding a $YO^{\bullet}$ component as in Equation S4.

Table S5. Optimized parameters of the fit of EADS4 (Y345F) according to Equation S3.

Spectrum	Parameter	Estimate	Standard error
EADS3	ϕ	0.81	0.003
$WH^{\bullet+}$	$a_1 \times 10^4$	2.81	0.02
	s_1 (nm)	-25	1
	k_1	0.926	0.002
$W^{\bullet}$	$a_2 \times 10^4$	1.79	0.03
	s_2 (nm)	78	2
	k_2	1.18	0.01

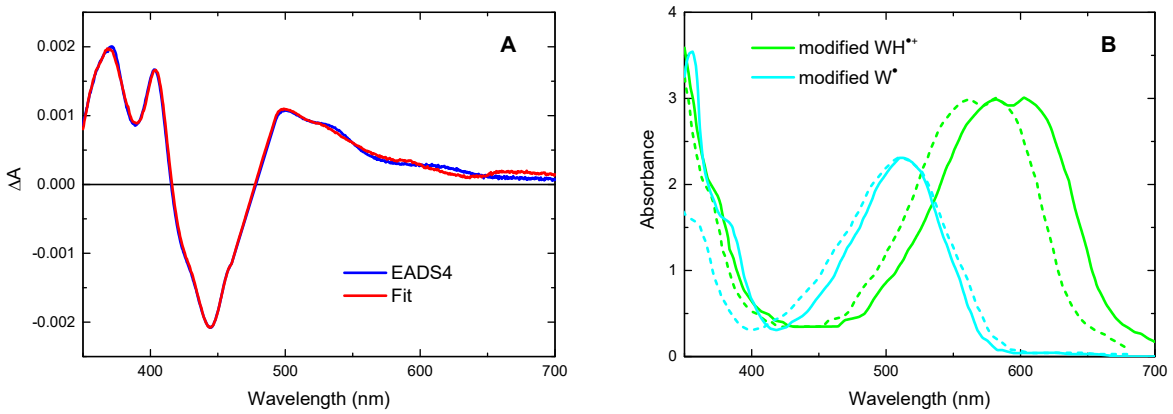

Figure S10. (A) Fit of EADS4 (Y345F) according to Equation S3. (B) Corresponding modified reference spectra (original spectra are recalled in dotted lines).

Supplementary references

1. J. Brazard, A. Usman, F. Lacombat, C. Ley, M. M. Martin, P. Plaza, L. Mony, M. Heijde, G. Zabulon and C. Bowler, *J. Am. Chem. Soc.*, 2010, **132**, 4935-4945.
2. R. Martin, F. Lacombat, A. Espagne, N. Dozova, P. Plaza, J. Yamamoto, P. Müller, K. Brettel and A. de la Lande, *Phys. Chem. Chem. Phys.*, 2017, **19**, 24493-24504.
3. P. Müller, E. Ignatz, S. Kiontke, K. Brettel and L. O. Essen, *Chem. Sci.*, 2018, **9**, 1200-1212.
4. J. Brazard, A. Usman, F. Lacombat, C. Ley, M. M. Martin and P. Plaza, *J. Phys. Chem. A*, 2011, **115**, 3251-3262.
5. J. Yamamoto, K. Shimizu, T. Kanda, Y. Hosokawa, S. Iwai, P. Plaza and P. Muller, *Biochemistry*, 2017, **56**, 5356-5364.
6. P. Macheroux, in *Flavoprotein Protocols*, eds. S. K. Chapman and G. A. Reid, 1999, pp. 1-7.
7. A. Berndt, T. Kottke, H. Breitkreuz, R. Dvorsky, S. Hennig, M. Alexander and E. Wolf, *J. Biol. Chem.*, 2007, **282**, 13011-13021.
8. S. Solar, N. Getoff, P. S. Surdhar, D. A. Armstrong and A. Singh, *J. Phys. Chem.*, 1991, **95**, 3639-3643.
9. C. Aubert, P. Mathis, A. P. M. Eker and K. Brettel, *Proc. Natl. Acad. Sci. USA*, 1999, **96**, 5423-5427.